



HAL
open science

Higher-Order Discontinuous Galerkin Method for Pyramidal Elements using Orthogonal Basis

Morgane Bergot, Marc Duruflé

► **To cite this version:**

Morgane Bergot, Marc Duruflé. Higher-Order Discontinuous Galerkin Method for Pyramidal Elements using Orthogonal Basis. 2010. hal-00547319v1

HAL Id: hal-00547319

<https://hal.science/hal-00547319v1>

Preprint submitted on 16 Dec 2010 (v1), last revised 13 Dec 2011 (v2)

HAL is a multi-disciplinary open access archive for the deposit and dissemination of scientific research documents, whether they are published or not. The documents may come from teaching and research institutions in France or abroad, or from public or private research centers.

L'archive ouverte pluridisciplinaire **HAL**, est destinée au dépôt et à la diffusion de documents scientifiques de niveau recherche, publiés ou non, émanant des établissements d'enseignement et de recherche français ou étrangers, des laboratoires publics ou privés.

HIGHER-ORDER DISCONTINUOUS GALERKIN METHOD FOR PYRAMIDAL ELEMENTS USING ORTHOGONAL BASIS

Morgane Bergot

Projet POems, INRIA Rocquencourt, Le Chesnay, France

Email: morgane.bergot@inria.fr

Marc Duruflé

Institut Mathématique de Bordeaux, Université Bordeaux I, Bordeaux, France

Email: marc.duruflé@math.u-bordeaux1.fr

Mathematics subject classification: 65F05, 65F50, 65M60, 65Y20

Abstract

We study arbitrarily high-order finite elements defined on pyramids for discontinuous Galerkin methods. We propose a new family of high-order pyramidal finite element using orthogonal basis functions which can be used in hybrid meshes including hexahedra, tetrahedra, wedges and pyramids. We perform a comparison between these orthogonal functions and nodal functions for affine and non-affine elements. Different strategies for the inversion of mass matrix are also considered and discussed. Numerical experiments are conducted for 3-D Maxwell's equations.

Key words: pyramidal element, higher-order finite element, hybrid mesh, conformal mesh, discontinuous Galerkin method, orthogonal basis functions.

Introduction

Discontinuous Galerkin methods have been extensively studied for tetrahedral meshes (e.g. Hesthaven and Warburton [1] for Maxwell's equations). Works of Cohen and collaborators (Fauqueux [2], Pernet and Ferrières [3], [4], Duruflé [5], [6]) have shown the higher efficiency obtained by using hexahedral meshes with this method, thanks to the tensorization of basis functions. However, generating high quality hexahedral meshes is not an easy task. A solution is to allow the insertion of other types of elements - tetrahedra, pyramids and triangular prisms with a high percentage of hexahedra - so that there is no loss in the efficiency.

Pyramidal elements have been studied by several authors in the context of continuous finite elements (Zaglmayr cited by Demkowicz in [7], Nigam and Phillips [8], [9], Bergot *et al.* [10], Sherwin *et al.* [11], Bluck and Walker [12], Wieners [13]) but their application to discontinuous Galerkin methods has received less attention. Obviously, basis functions developed for continuous finite elements can be used for discontinuous elements as it is achieved in [10]. However, since continuity is not required, other sets of basis functions are acceptable and may have better properties. An attractive choice consists of orthogonal basis, which has been proposed by Kirby *et al.* [14] for all the types of elements, but the proposed basis functions for pyramids generate \mathbb{P}_r instead of the optimal finite element space. We illustrate here that the use of \mathbb{P}_r for pyramids provides a poor convergence for non-affine pyramids. A recent work of Gassner *et al.* [15] proposes an original approach to construct nodal discontinuous Galerkin method for hybrid meshes, since it avoids the use of a reference element, by constructing directly nodal functions generating polynomials on the real element.

We consider linear hyperbolic problems like Maxwell's equations, with an explicit time scheme (like Runge-Kutta). Continuous Galerkin finite element schemes are not attractive in this context, since the mass matrix is large and costly to invert. Mass-lumped elements are well-known for hexahedra (Cohen [16]), but less mastered for other elements (see Mulder et al. [17] for tetrahedra) and the proposed elements require a large number of additional degrees of freedoms and lead to a more restrictive stability condition. Furthermore, the application of a continuous Galerkin formulation is tedious because of spurious modes: it often needs regularization, as described by Costabel in [18] for Maxwell's equations. When a discontinuous Galerkin method is considered, nonetheless we get a block-diagonal mass matrix, but orthogonal tensorized basis functions can be used to get elementary sparse mass matrix, which induces a gain in computational time when the order of approximation is large enough.

In this paper, we propose orthogonal tensorized basis functions generating optimal finite element spaces for non-affine hexahedra, prisms, pyramids, and orthogonal basis functions generating polynomials \mathbb{P}_r for affine elements. These two sets of basis functions are compared on the special case of affine elements, and it appears that the orthogonal basis functions generating optimal finite element spaces are more efficient. Several solutions to construct and invert the mass matrix are considered and compared, and a fast algorithm to compute the mass matrix for the pyramidal element is detailed. The fast matrix-vector product algorithm obtained because of tensorization of orthogonal basis functions is also given for all types of elements, the complexity of such a matrix-vector product is in $O(r^4)$ where r is the order of approximation, instead of $O(r^6)$ when no tensorization is available (e.g. nodal functions of the pyramid). Therefore orthogonal functions are asymptotically more efficient than nodal functions, but it has been numerically found that it was more efficient for pyramids from $r \geq 3$, for wedges from $r \geq 5$ and for tetrahedra from $r \geq 10$. Finally, numerical results are provided for the resolution of 3-D time-domain Maxwell's equations.

The outline of our paper is as follows:

- In Section 1, we present the representative problem we study and its discretization in space and in time.
- We detail in Section 2 the construction of the mass matrix for pyramidal elements, when using classical nodal basis functions in Section 2.1 and orthogonal basis functions in Section 2.2. A way to obtain a diagonal mass matrix, proposed by Warburton (ICOSAHOM 09) is considered in Section 2.3.
- Section 3 is devoted to the construction of a fast matrix-vector product using orthogonal basis functions.
- We perform numerical comparisons of several types of elements in Section 4
- In Section 5, we consider numerical applications on 3-D time-domain Maxwell's equations.

1. Definitions and Presentation of the Problem

1.1. Definitions and Variational Formulation

We consider the following representative linear hyperbolic problem (e.g. Godlewski and Raviart [19])

$$M \frac{\partial u}{\partial t} + \sum_{1 \leq i \leq d} A_i \frac{\partial u}{\partial x_i} + \sum_{1 \leq i \leq d} B_i \frac{\partial u}{\partial x_i} = 0, \quad (M, A_i, B_i) \in (\mathcal{M}_{n_s}(\mathbb{R}))^3, u \in \mathbb{R}^{n_s} \quad (1.1)$$

where n_s is the number of scalar unknowns of the equation, and d is the dimension. When the system is symmetric,

$$B_i = A_i^*.$$

Remark 1.1. *This formulation is useful to exhibit the antisymmetry of the stiffness matrix when using centered flux and without absorbing conditions, which is essential to get the stability.*

Let Ω be an open set of \mathbb{R}^3 , composed of n_e elements K_i

$$\Omega = \bigcup_{1 \leq i \leq n_e} K_i.$$

For any element K of boundary ∂K of outward normal n , we consider a discontinuous method. For example, the Local Discontinuous Galerkin (LDG) formulation (see Hesthaven and Warburton [20] for Maxwell's equations) writes

$$\left\{ \begin{array}{l} \text{Find } u \in V \text{ such that} \\ \forall v \in V, \quad \frac{d}{dt} \int_K M u \cdot v \, dx - \int_K \sum_{1 \leq i \leq d} \left(A_i u \cdot \frac{\partial v}{\partial x_i} - B_i \frac{\partial u}{\partial x_i} \cdot v \right) dx \\ \quad \quad \quad + \int_{\partial K} (N_1 \{u\} + N_2 [u]) \cdot v \, ds = 0, \end{array} \right. \quad (1.2)$$

where $V = (L^2(\Omega))^{n_s}$, $N_1 = \sum_{1 \leq i \leq d} A_i n_i$, $N_2 = \sum_{1 \leq i \leq d} B_i n_i$. The average $\{u\}$ is

$$\{u\} = \frac{1}{2}(u_1 + u_2)$$

and $[u]$ is

$$[u] = \frac{1}{2}(u_2 - u_1) + \frac{1}{2}\alpha \int_{\partial K} C(u_2 - u_1) \, ds,$$

where C is a symmetric positive matrix, u_1 value of u on the element K and u_2 value of u on a neighbour element of K , and $\alpha \leq 0$. In general, we take $\alpha = -0.5$ in our experiments.

1.2. Space Discretization

Given a finite-dimension subspace V_h of the space V , the discrete problem reads

$$\left\{ \begin{array}{l} \text{Find } u_h \in V_h \text{ such that} \\ \forall v_h \in V_h, \quad \frac{d}{dt} \int_K M u_h \cdot v_h \, dx - \int_K \sum_{1 \leq i \leq d} \left(A_i u_h \cdot \frac{\partial v_h}{\partial x_i} - B_i \frac{\partial u_h}{\partial x_i} \cdot v_h \right) dx \\ \quad \quad \quad + \int_{\partial K} (N_1 \{u_h\} + N_2 [u_h]) \cdot v_h \, ds = 0. \end{array} \right. \quad (1.3)$$

We note by $n = n_s n_r$ the dimension of V_h .

To write the integrals on the reference element, the standard transformation (Ciarlet [21]) F from a reference element \hat{K} to the mesh element K for hexahedral, tetrahedral and wedge elements is used. For pyramidal elements, following Bedrosian [22], we define a transformation using rational fractions.

Definition 1.1. *The transformation F from the reference pyramid $\hat{K}(\hat{x}, \hat{y}, \hat{z})$ taken as the unit symmetrical pyramid, centered at the origin (see Fig. 1.1) to a pyramid $K(x, y, z)$ of vertices $S_i = (x_i, y_i, z_i)$ is*

$$4F = (S_1 + S_2 + S_3 + S_4) + \hat{x}(-S_1 + S_2 + S_3 - S_4) + \hat{y}(-S_1 - S_2 + S_3 + S_4) + \hat{z}(4S_5 - S_1 - S_2 - S_3 - S_4) + \frac{\hat{x}\hat{y}}{1-\hat{z}}(S_1 + S_3 - S_2 - S_4). \quad (1.4)$$

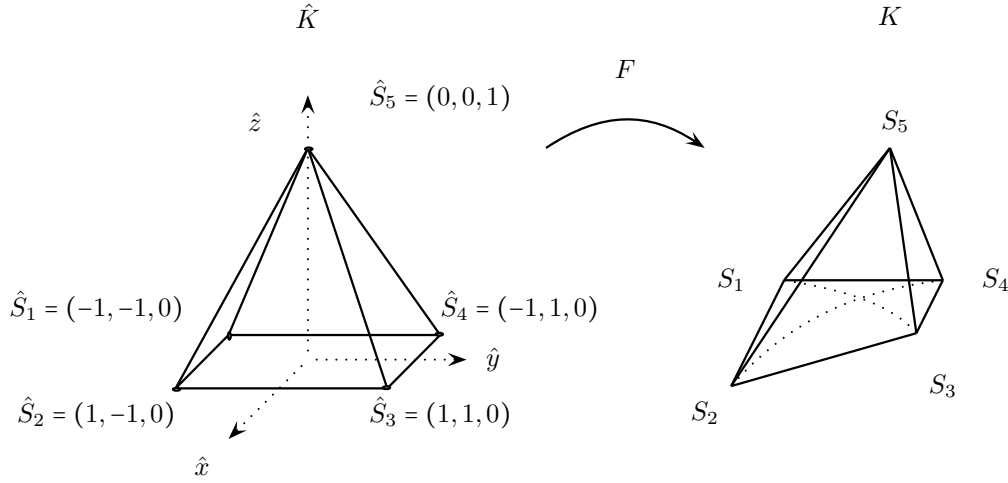


Fig. 1.1. Transformation of the reference pyramid \hat{K} to the pyramid K via the transformation F

Remark 1.2. *The case of a non-invertible transformation may occur when considering a degenerated element, e.g. when the five vertices are co-planar. The characterisation of pyramids for which F is invertible remains an still open question, as for hexahedra (Duruflé et al. [6]). In the sequel, we assume that F is always invertible.*

The finite element space V_h on Ω is given by

$$V_h = \left\{ u \in L^2(\Omega) \mid u|_K \in (\mathbb{P}_r^F(K))^{n_s} \right\},$$

where \mathbb{P}_r^F is the real space of order r for an element K of the mesh defined by

$$\mathbb{P}_r^F(K) = \left\{ u \mid u \circ F \in (\hat{P}_r(\hat{K}))^{n_s} \right\}.$$

The finite element space \hat{P}_r of order r on the reference element \hat{K} is

- *Tetrahedron:* $\mathbb{P}_r(\hat{x}, \hat{y}, \hat{z}) = \{ \hat{x}^i \hat{y}^j \hat{z}^k, i + j + k \leq r \}$ of dimension $n_r = \frac{(r+1)(r+2)(r+3)}{6}$, and \hat{K} is the unit tetrahedron $0 \leq \hat{x} + \hat{y} + \hat{z} \leq 1$;

- *Hexahedron*: $\mathbb{Q}_r(\hat{x}, \hat{y}, \hat{z}) = \{\hat{x}^i \hat{y}^j \hat{z}^k, i, j, k \leq r\}$ of dimension $n_r = (r+1)^3$, and \hat{K} is the unit cube $[0, 1]^3$;
- *Wedge*: $\mathbb{P}_r(\hat{x}, \hat{y}) \otimes \mathbb{P}_r(\hat{z}) = \{\hat{x}^i \hat{y}^j \hat{z}^k, i+j \leq r, k \leq r\}$ of dimension $n_r = \frac{(r+1)^2(r+2)}{2}$, and \hat{K} is the unit wedge $0 \leq \hat{x} + \hat{y}, \hat{z} \leq 1$;
- *Pyramid*: $\mathbb{P}_r(\hat{x}, \hat{y}, \hat{z}) \oplus \sum_{0 \leq k \leq r-1} \left(\frac{\hat{x}\hat{y}}{1-\hat{z}}\right)^{r-k} \mathbb{P}_k(\hat{x}, \hat{y})$ of dimension $n_r = \frac{(r+1)(r+2)(2r+3)}{6}$, when \hat{K} is the unit symmetrical pyramid, centered at the origin.

The finite element space is classical for tetrahedra, hexahedra and wedges (Ciarlet [21]) but is less standard in the case of a pyramidal element.

This choice of finite element space is optimal, that is by choosing this finite element space, the final error estimate is in $O(h^{r+1})$ in L^2 -norm, whereas choosing any subspace included in this one leads to a convergence of at most $O(h^r)$ (see [10]). This can be seen by displaying the dispersion error (see Cohen [16] for an explanation of how to perform a dispersion analysis) on a periodic mesh containing non-affine pyramids, whose cell is presented on Fig. 1.2. As shows Fig. 1.3 displaying the dispersion error obtained for Maxwell's equations, using the optimal finite element space provides a dispersion error in $O(h^{2r+1})$ (see Pernet [23] for the factor $2r+1$), whereas the use of \mathbb{P}_r as for tetrahedra leads to a low convergence rate.

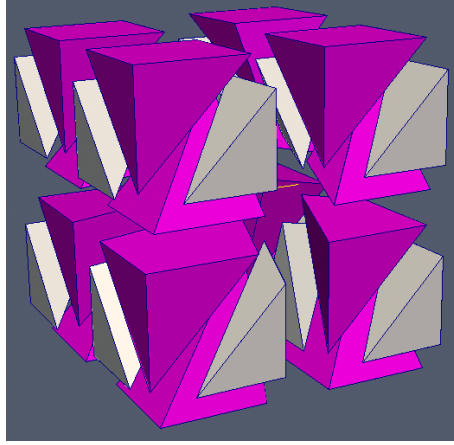


Fig. 1.2. Periodic pattern for the hybrid case, with distorted pyramids (purple) and tetrahedra (gray)

Definition 1.2. Let $(\varphi_i)_{i \leq n_r}$ be a base of V_h , let M_h the mass matrix for the pyramid K , defined by

$$(M_h)_{i,j} = \int_K M \varphi_i \cdot \varphi_j dx \quad (1.5)$$

the stiffness matrix R_h such that

$$(R_h)_{i,j} = \int_K \sum_{1 \leq k \leq d} \left(A_k \frac{\partial \varphi_i}{\partial x_k} \cdot \varphi_j - B_k \varphi_i \cdot \frac{\partial \varphi_j}{\partial x_k} \right) dx \quad (1.6)$$

and the flux matrix S_h defined by

$$(S_h)_{i,j} = \int_{\partial K} \sum_{1 \leq k \leq d} (N_1 \{\varphi_j\} + N_2 [\varphi_j]) \cdot \varphi_i ds. \quad (1.7)$$

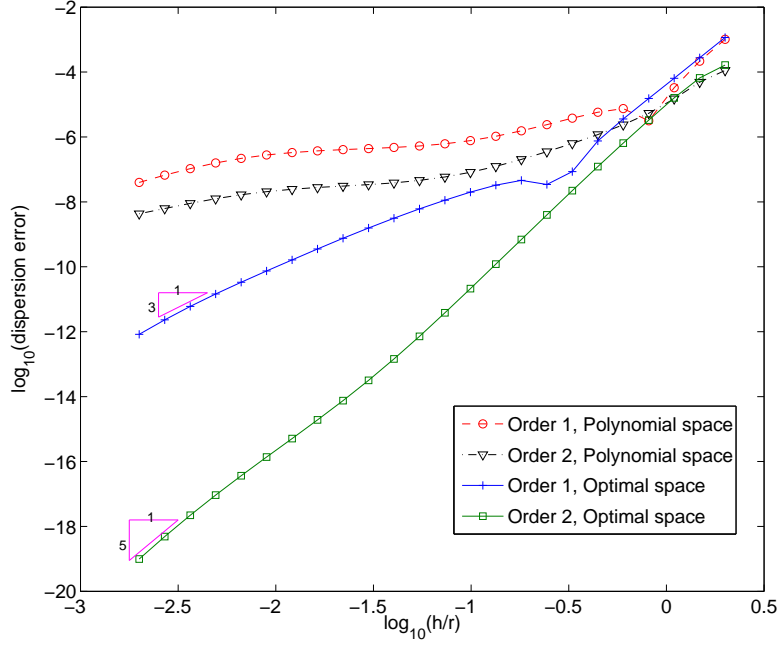


Fig. 1.3. Dispersion error for a periodic mesh with non-affine pyramids for Maxwell's equation

The space discretization then writes

$$\frac{d}{dt}M_h U - R_h U + S_h U = 0, \quad (1.8)$$

1.3. Time Discretization

Using any explicit time scheme, for example the low-storage Runge-Kutta scheme of order 4 (Carpenter and Kennedy [24]), the time discretization writes

$$\begin{aligned} U^{n+1} &= U^n \\ \rho &= U^n \\ \text{for } i &= 1 \text{ to } 5 \\ \rho &= \alpha_i \rho + \Delta t (M_h)^{-1} (R_h - S_h)(U^{n+1}) \\ U^{n+1} &= U^{n+1} + \beta_i \rho \\ \text{end for} \end{aligned} \quad (1.9)$$

For each time-step, we then have to

- compute the matrix-vector products $R_h U^n$ and $S_h U^n$;
- solve a linear system $(M_h) X = Y$;

We first present an efficient technique to construct M_h and solve the linear system for pyramidal elements.

2. Mass Matrix

2.1. Dense Mass Matrix with Nodal Basis Functions

Using the H^1 -conforming transformation (Monk [25]) of the basis functions from any element K of the mesh to the reference element \hat{K}

$$\hat{\varphi}_i = \varphi_i \circ F^{-1}, \quad (2.1)$$

the mass matrix writes

$$(M_h)_{i,j} = \int_K M \varphi_i \varphi_j \, dx \, dy \, dz = \int_{\hat{K}} M |DF| \hat{\varphi}_i \hat{\varphi}_j \, d\hat{x} \, d\hat{y} \, d\hat{z}. \quad (2.2)$$

The nodal basis functions on the reference element \hat{K} are obtained by inverting a Vandermonde system as follow. Let $(\hat{M}_i)_{1 \leq i \leq n_r}$ the locations of the interpolation points on the pyramid (see [10] for the choice of their location), and $(\hat{\psi}_i)_{1 \leq i \leq n_r}$ a base of \hat{P}_r ,

Definition 2.1. *The Vandermonde matrix $VDM \in \mathcal{M}_{n_r}(\mathbb{R})$ is defined by*

$$VDM_{i,j} = \hat{\psi}_i(\hat{M}_j), \quad 1 \leq i, j \leq n_r,$$

and the basis function $\hat{\varphi}_i$ linked to the interpolation point \hat{M}_i is then defined as

$$\hat{\varphi}_i = \sum_{1 \leq j \leq n_r} (VDM^{-1})_{i,j} \hat{\psi}_j.$$

Remark 2.1. *The characterisation of the invertibility of the Vandermonde matrix is an open question, but we observed that the VDM matrix is invertible with our choice of position for the degrees of freedom, the element is therefore unisolvent.*

As it can be found in [10], the use of an orthogonal base of \hat{P}_r for $(\hat{\psi}_i)_{1 \leq i \leq n_r}$ decreases the condition number of the Vandermonde matrix compared to the monomial base of \hat{P}_r . However, the mass matrix is dense and has no particular property.

2.2. Sparse Mass Matrix with Orthogonal Basis Functions

2.2.1. Orthogonal Basis Functions

When using orthogonal basis functions, we expect to have a sparser mass matrix than with nodal functions.

We denote by $P_m^{i,j}(x)$ the orthonormalized Jacobi polynomial of order m , orthogonal for the weight $(1-x)^i(1+x)^j$, and ξ_j^G the points of Gauss-Legendre on $[0, 1]$ (cf Hammer, Marlowe and Stroud [26]).

Proposition 2.1. *The following set of basis functions is an orthogonal base of \hat{P}_r*

- **Hexahedron**

$$\hat{\varphi}_{i_1}^G(\hat{x}) \hat{\varphi}_{i_2}^G(\hat{y}) \hat{\varphi}_{i_3}^G(\hat{z}), \quad 0 \leq i_1, i_2, i_3 \leq r,$$

where

$$\hat{\varphi}_i^G(\hat{x}) = \frac{\prod_{j \neq i} \hat{x} - \xi_j^G}{\prod_{j \neq i} \xi_i^G - \xi_j^G},$$

- **Wedge**

$$P_{i_1}^{0,0} \left(\frac{2\hat{x}}{1-\hat{y}} - 1 \right) (1-\hat{y})^{i_1} P_{i_2}^{2i_1+1,0} (2\hat{y}-1) \varphi_{i_3}^G(\hat{z}), \quad 0 \leq i_1 + i_2, i_3 \leq r,$$

- **Pyramid**

$$P_{i_1}^{0,0} \left(\frac{\hat{x}}{1-\hat{z}} \right) P_{i_2}^{0,0} \left(\frac{\hat{y}}{1-\hat{z}} \right) (1-\hat{z})^{\max(i_1, i_2)} P_{i_3}^{2\max(i_1, i_2)+2,0} (2\hat{z}-1), \\ 0 \leq i_1, i_2 \leq r, 0 \leq i_3 \leq r - \max(i_1, i_2),$$

- **Tetrahedron**

$$P_{i_1}^{0,0} \left(\frac{2\hat{x}}{1-\hat{y}-\hat{z}} - 1 \right) P_{i_2}^{2i_1+1,0} \left(\frac{2\hat{y}}{1-\hat{z}} - 1 \right) (1-\hat{y}-\hat{z})^{i_1} P_{i_3}^{2(i_1+i_2)+2,0} (2\hat{z}-1) (1-\hat{z})^{i_2}, \\ 0 \leq i_1 + i_2 + i_3 \leq r.$$

Proof. See Proposition 1.10 in [10] for pyramidal elements. Proof is similar for the other types of elements.

When the element is affine, we can use $\hat{P}_r = \mathbb{P}_r$ (see Theorem 1.4 in [10]).

Proposition 2.2. *The following set of basis functions is an orthogonal base of \mathbb{P}_r*

For $0 \leq i_1 + i_2 + i_3 \leq r$,

- **Hexahedron**

$$P_{i_1}^{0,0} (2\hat{x}-1) P_{i_2}^{0,0} (2\hat{y}-1) P_{i_3}^{0,0} (2\hat{z}-1),$$

- **Wedge**

$$P_{i_1}^{0,0} \left(\frac{2\hat{x}}{1-\hat{y}} - 1 \right) (1-\hat{y})^{i_1} P_{i_2}^{2i_1+1,0} (2\hat{y}-1) \varphi_{i_3}^G(\hat{z}),$$

- **Pyramid**

$$P_{i_1}^{0,0} \left(\frac{\hat{x}}{1-\hat{z}} \right) P_{i_2}^{0,0} \left(\frac{\hat{y}}{1-\hat{z}} \right) (1-\hat{z})^{i_1+i_2} P_{i_3}^{2(i_1+i_2)+2,0} (2\hat{z}-1),$$

- **Tetrahedron**

$$P_{i_1}^{0,0} \left(\frac{2\hat{x}}{1-\hat{y}-\hat{z}} - 1 \right) P_{i_2}^{2i_1+1,0} \left(\frac{2\hat{y}}{1-\hat{z}} - 1 \right) (1-\hat{y}-\hat{z})^{i_1} P_{i_3}^{2(i_1+i_2)+2,0} (2\hat{z}-1) (1-\hat{z})^{i_2}.$$

Proof. Proof is similar to the proof of Proposition 2.1.

2.2.2. Fast Algorithm for Pyramidal Elements

We use the orthogonal base of \hat{P}_r defined in Proposition 2.1 as set of basis functions to make the matrix sparser. To make the computation easier, we write the integrals on the unit cube \tilde{Q} . We first define the transformation T from the unit cube \tilde{Q} on the reference pyramid \hat{K}

$$T : \begin{cases} \hat{x} = (1-\tilde{z})(2\tilde{x}-1) \\ \hat{y} = (1-\tilde{z})(2\tilde{y}-1) \\ \hat{z} = \tilde{z}. \end{cases} \quad (2.3)$$

For any function f , we denote

$$\tilde{f}(\tilde{x}, \tilde{y}, \tilde{z}) = f(\hat{x}, \hat{y}, \hat{z}),$$

and the change of variable provides

$$\int_{\tilde{K}} \hat{f}(\hat{x}, \hat{y}, \hat{z}) d\hat{x} d\hat{y} d\hat{z} = \int_{\tilde{Q}} 4 \tilde{f}(\tilde{x}, \tilde{y}, \tilde{z}) (1 - \tilde{z})^2 d\tilde{x} d\tilde{y} d\tilde{z}. \quad (2.4)$$

The mass matrix written on the unit cube \tilde{Q} is then

$$(M_h)_{i,j} = 4 \int_{\tilde{Q}} M |\widetilde{DF}| \tilde{\varphi}_i \tilde{\varphi}_j (1 - \tilde{z})^2 d\tilde{x} d\tilde{y} d\tilde{z},$$

where the jacobian $|DF|$ of the transformation F on the unit cube \tilde{Q} can be written as (see Lemma 3.5 in [10])

$$|\widetilde{DF}| = A + B_1(2\tilde{x} - 1) + B_2(2\tilde{y} - 1) + C(2\tilde{x} - 1)(2\tilde{y} - 1).$$

We recall the following property of Jacobi polynomial (Szegö [27])

Property 2.1.

$$tP_k^{i,j}(t) = \gamma_k^{i,j} P_{k+1}^{i,j}(t) + \alpha_k^{i,j} P_k^{i,j}(t) + \beta_k^{i,j} P_{k-1}^{i,j}(t), \quad (2.5)$$

where

$$\begin{aligned} \alpha_k^{i,j} &= -a_{i,j,k} \frac{(2k+i+j)(i^2-j^2)}{2k+i+j} \\ \beta_k^{i,j} &= b_{i,j,k} \frac{2(k+i)(k+j)(2k+i+j+2)}{2k+i+j} \\ \gamma_k^{i,j} &= c_{i,j,k} 2(k+1)(k+i+j+1) \end{aligned}$$

and $a_{i,j,k}$, $b_{i,j,k}$ and $c_{i,j,k}$ are coefficients due to orthonormalisation of Jacobi polynomial $P_k^{i,j}$.

Using Property 2.1, we decompose the mass matrix as follows, for all $i = (i_1, i_2, i_3)$, $1 \leq i \leq n_r$ and for all j_3 , $0 \leq j_3 \leq r$

- Term in A :

$$\begin{aligned} \int_{\tilde{Q}} \tilde{\varphi}_i \tilde{\varphi}_j (1 - \tilde{z})^2 d\tilde{x} d\tilde{y} d\tilde{z} &= \\ &\underbrace{\int_0^1 P_{i_1}^{0,0}(2\tilde{x}-1) P_{j_1}^{0,0}(2\tilde{x}-1) d\tilde{x}}_{\delta_{i_1 j_1}} \\ &\underbrace{\int_0^1 P_{i_2}^{0,0}(2\tilde{y}-1) P_{j_2}^{0,0}(2\tilde{y}-1) d\tilde{y}}_{\delta_{i_2 j_2}} \\ &\underbrace{\int_0^1 (1 - \tilde{z})^{\max(i_1, i_2) + \max(j_1, j_2) + 2} P_{i_3}^{2\max(i_1, i_2) + 2, 0}(2\tilde{z}-1) P_{j_3}^{2\max(j_1, j_2) + 2, 0}(2\tilde{z}-1) d\tilde{z}}_{\delta_{i_3 j_3}} \end{aligned}$$

- Term in B_1 :

$$\begin{aligned}
& \int_{\tilde{Q}} \tilde{\varphi}_i \tilde{\varphi}_j (2\tilde{x} - 1)(1 - \tilde{z})^2 d\tilde{x} d\tilde{y} d\tilde{z} = \\
& \underbrace{\int_0^1 (2\tilde{x} - 1) P_{i_1}^{0,0}(2\tilde{x} - 1) P_{j_1}^{0,0}(2\tilde{x} - 1) d\tilde{x}}_{\gamma_{i_1}^{0,0} \delta_{i_1+1j_1} + \beta_{i_1}^{0,0} \delta_{i_1-1j_1}} \\
& \underbrace{\int_0^1 P_{i_2}^{0,0}(2\tilde{y} - 1) P_{j_2}^{0,0}(2\tilde{y} - 1) d\tilde{y}}_{\delta_{i_2j_2}} \\
& \underbrace{\int_0^1 (1 - \tilde{z})^{\max(i_1, i_2) + \max(j_1, j_2) + 2} P_{i_3}^{2\max(i_1, i_2) + 2, 0}(2\tilde{z} - 1) P_{j_3}^{2\max(j_1, j_2) + 2, 0}(2\tilde{z} - 1) d\tilde{z}}_{\mathbb{C}_{i_1, j_1}^{i_2, j_2}(i_3, j_3)};
\end{aligned}$$

- Term in B_2 :

$$\begin{aligned}
& \int_{\tilde{Q}} \tilde{\varphi}_i \tilde{\varphi}_j (2\tilde{y} - 1)(1 - \tilde{z})^2 d\tilde{x} d\tilde{y} d\tilde{z} = \\
& \underbrace{\int_0^1 P_{i_1}^{0,0}(2\tilde{x} - 1) P_{j_1}^{0,0}(2\tilde{x} - 1) d\tilde{x}}_{\delta_{i_1j_1}} \\
& \underbrace{\int_0^1 (2\tilde{y} - 1) P_{i_2}^{0,0}(2\tilde{y} - 1) P_{j_2}^{0,0}(2\tilde{y} - 1) d\tilde{y}}_{\gamma_{i_2}^{0,0} \delta_{i_2+1j_2} + \beta_{i_2}^{0,0} \delta_{i_2-1j_2}} \\
& \underbrace{\int_0^1 (1 - \tilde{z})^{\max(i_1, i_2) + \max(j_1, j_2) + 2} P_{i_3}^{2\max(i_1, i_2) + 2, 0}(2\tilde{z} - 1) P_{j_3}^{2\max(j_1, j_2) + 2, 0}(2\tilde{z} - 1) d\tilde{z}}_{\mathbb{C}_{i_1, j_1}^{i_2, j_2}(i_3, j_3)};
\end{aligned}$$

- Term in C :

$$\begin{aligned}
& \int_{\tilde{Q}} \tilde{\varphi}_i \tilde{\varphi}_j (2\tilde{x} - 1)(2\tilde{y} - 1)(1 - \tilde{z})^2 d\tilde{x} d\tilde{y} d\tilde{z} = \\
& \underbrace{\int_0^1 (2\tilde{x} - 1) P_{i_1}^{0,0}(2\tilde{x} - 1) P_{j_1}^{0,0}(2\tilde{x} - 1) d\tilde{x}}_{\gamma_{i_1}^{0,0} \delta_{i_1+1j_1} + \beta_{i_1}^{0,0} \delta_{i_1-1j_1}} \\
& \underbrace{\int_0^1 (2\tilde{y} - 1) P_{i_2}^{0,0}(2\tilde{y} - 1) P_{j_2}^{0,0}(2\tilde{y} - 1) d\tilde{y}}_{\gamma_{i_2}^{0,0} \delta_{i_2+1j_2} + \beta_{i_2}^{0,0} \delta_{i_2-1j_2}} \\
& \underbrace{\int_0^1 (1 - \tilde{z})^{\max(i_1, i_2) + \max(j_1, j_2) + 2} P_{i_3}^{2\max(i_1, i_2) + 2, 0}(2\tilde{z} - 1) P_{j_3}^{2\max(j_1, j_2) + 2, 0}(2\tilde{z} - 1) d\tilde{z}}_{\mathbb{C}_{i_1, j_1}^{i_2, j_2}(i_3, j_3)}.
\end{aligned}$$

That is, the mass matrix is computed as follows, for all $i = (i_1, i_2, i_3)$, $1 \leq i \leq n_r$ and for all j_3 , $0 \leq j_3 \leq r$

- $M_h[i, i] = A$
- $M_h[i, (i_1 + 1, i_2, j_3)] = B_1 \gamma_{i_1}^{0,0} \mathbb{C}_{i_1, i_1+1}^{i_2, i_2}(i_3, j_3)$

- $M_h[i, (i_1 - 1, i_2, j_3)] = B_1 \beta_{i_1}^{0,0} \mathcal{C}_{i_1, i_1 - 1}^{i_2, i_2}(i_3, j_3)$
- $M_h[i, (i_1, i_2 + 1, j_3)] = B_2 \gamma_{i_2}^{0,0} \mathcal{C}_{i_1, i_1}^{i_2, i_2 + 1}(i_3, j_3)$
- $M_h[i, (i_1, i_2 - 1, j_3)] = B_2 \beta_{i_2}^{0,0} \mathcal{C}_{i_1, i_1}^{i_2, i_2 - 1}(i_3, j_3)$
- $M_h[i, (i_1 + 1, i_2 + 1, j_3)] = C \gamma_{i_1}^{0,0} \mathcal{C}_{i_1, i_1 + 1}^{i_2, i_2}(i_3, j_3) \gamma_{i_2}^{0,0} \mathcal{C}_{i_1, i_1}^{i_2, i_2 + 1}(i_3, j_3)$
- $M_h[i, (i_1 + 1, i_2 - 1, j_3)] = C \gamma_{i_1}^{0,0} \mathcal{C}_{i_1, i_1 + 1}^{i_2, i_2}(i_3, j_3) \beta_{i_2}^{0,0} \mathcal{C}_{i_1, i_1}^{i_2, i_2 - 1}(i_3, j_3)$
- $M_h[i, (i_1 - 1, i_2 + 1, j_3)] = C \beta_{i_1}^{0,0} \mathcal{C}_{i_1, i_1 - 1}^{i_2, i_2}(i_3, j_3) \gamma_{i_2}^{0,0} \mathcal{C}_{i_1, i_1}^{i_2, i_2 + 1}(i_3, j_3)$
- $M_h[i, (i_1 - 1, i_2 - 1, j_3)] = C \beta_{i_1}^{0,0} \mathcal{C}_{i_1, i_1 - 1}^{i_2, i_2}(i_3, j_3) \beta_{i_2}^{0,0} \mathcal{C}_{i_1, i_1}^{i_2, i_2 - 1}(i_3, j_3)$

The mass matrix contains $O(r^4)$ non-zero entries instead of $O(r^6)$, and integrals $\mathcal{C}_{i_1, j_1}^{i_2, j_2}(i_3, j_3)$ are precomputed. The cost of computation is finally in $O(r^4)$.

To solve the linear system, we use a LU factorisation. In the sparse case, the profile of the mass matrix can be improved to decrease the storage in the LU factorisation. For example, with our first choice of numbering, we used the Symmetric Approximate Minimum Degree permutations (symamd) algorithm, developed by Amestoy *et al.* in [28]. The result is shown in Fig. 2.1. In this case, for order 2, the profile of the mass matrix is 21% smaller, 34% at order 3, 54% at order 5 and 70% at order 8.

2.2.3. Mass Matrix for the Other Elements

With the mass-lumping, the mass matrix is diagonal for hexahedral elements. For tetrahedral elements, as the jacobian is constant, the mass matrix is also diagonal when using orthogonal basis functions.

For wedge elements, as we have tensorisation and mass-lumping in z , the mass matrix is already block diagonal on each element, even for nodal elements for which the number of non-zero entries is in $O(r^5)$. Using orthogonal basis functions make each block sparser, but the gain is far less spectacular than for pyramidal elements. The same algorithm as for pyramidal elements could also be used for wedge elements to fasten the computation, but is not presented here.

2.3. Diagonal Mass Matrix with Warburton's Trick

In the discontinuous case, the resolution of the linear system can be avoided by using the following non- H^1 -conforming transformation

$$\hat{\varphi}_i = \frac{1}{\sqrt{|DF|}} \varphi_i \circ F^{-1}. \quad (2.6)$$

Using this transformation on the reference element, the mass matrix writes

$$(M_h)_{i,j} = \int_K \varphi_i \cdot \varphi_j dx = \int_{\hat{K}} |DF| \frac{\hat{\varphi}_i}{\sqrt{|DF|}} \cdot \frac{\hat{\varphi}_j}{\sqrt{|DF|}} dx = \int_{\hat{K}} \hat{\varphi}_i \cdot \hat{\varphi}_j dx,$$

that is the mass matrix is independent of the geometry. If orthonormal basis functions are used, the matrix is equal to identity.

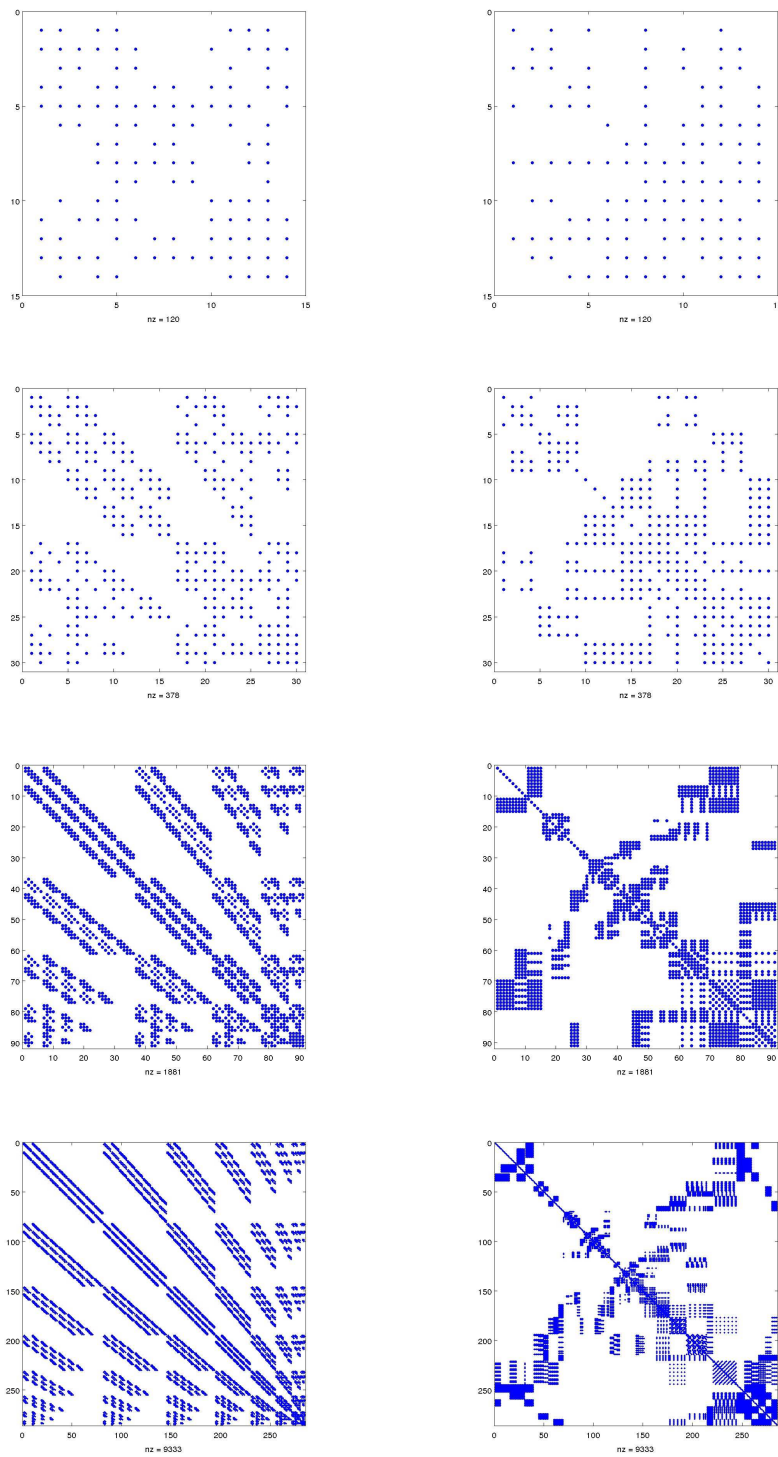


Fig. 2.1. Profile of the mass matrices of order 2, 3, 5 and 8 before (left) and after (right) renumbering, with an symamd algorithm

3. Fast Matrix-Vector Product

3.1. Introduction

In the time discretization (see algorithm 1.9), a needed step consists of performing the following matrix-vector product

$$y^n = (R_h - S_h) U^n$$

Storing the matrix $R_h - S_h$ as a sparse matrix and performing a standard matrix-vector product would be an expensive solution as the memory required to store such a large matrix may become too important, especially when high order is used.

Since inside each element (except hexahedron), all the degrees of freedom are interacting with each other, i.e.

$$\int_K \frac{\partial \varphi_k}{\partial x_i} \varphi_j \neq 0, \quad \forall j, k$$

the number of non-zero entries in matrix $R_h - S_h$ is equal to $O(n_e r^6)$ where n_e is the number of elements in the mesh and r the order of approximation. The computational time required for the matrix-vector product would therefore be in $O(n_e r^6)$ too if the matrix $R_h - S_h$ is stored.

Another solution, well-known for tetrahedra (Hesthaven [1]) consists in performing the matrix-vector product without storing the matrix. For nodal basis functions, the computational time will remain in $O(n_e r^6)$, whereas for orthogonal functions, the tensorization of basis functions induce fast algorithms in $O(n_e r^4)$ as pointed out in Warburton's thesis [29].

In the following section, we detail an efficient algorithm for the discontinuous Galerkin formulation used in this paper.

3.2. H^1 -conforming Transformation

3.2.1. General Method

We are considering the following matrix vector product

$$y_j = \int_K \sum_{1 \leq i \leq d} \left(A_i U \cdot \frac{\partial \varphi_j}{\partial x_i} - B_i \frac{\partial U}{\partial x_i} \cdot \varphi_j \right) dx - \int_{\partial K} (N_1 \{U\} + N_2 [U]) \cdot \varphi_j ds$$

We use F^{-1} to transform any element K of the mesh into the reference element \hat{K} , and T defined by equation 2.3 to transform the reference pyramid \hat{K} into the unit cube \tilde{Q} . Let us denote by $G = F \circ T$, the transformation from the pyramid K into the unit cube \tilde{Q} . We also use a transformation g^{-1} from a face ∂K to a reference face $\partial \tilde{Q}$. As

$$\tilde{u} = \sum_k \tilde{u}_k \tilde{\varphi}_k,$$

y_j finally writes

$$y_j = \int_{\tilde{Q}} |\overline{DG}| \sum_{1 \leq i \leq d} \sum_{1 \leq l \leq d} \left(A_i \tilde{u} \cdot (\overline{DG}^{-1})_{l,i} \frac{\partial \tilde{\varphi}_j}{\partial \tilde{x}_l} - B_i (\overline{DG}^{-1})_{l,i} \frac{\partial \tilde{u}}{\partial \tilde{x}_l} \cdot \tilde{\varphi}_j \right) d\tilde{x} d\tilde{y} d\tilde{z} \\ - \int_{\partial \tilde{Q}} |\overline{Dg}| (N_1 \{\tilde{u}\} + N_2 [\tilde{u}]) \cdot \tilde{\varphi}_j d\tilde{s}.$$

Volume integrals are evaluated with quadrature formulas (ω_m, ξ_m) , suited for the cube \tilde{Q} , whereas surface integrals are evaluated with quadrature formulas (ω'_n, ξ'_n) suited for the faces of cube $\partial \tilde{Q}$. Let us define

$$\bar{U} = - (N_1 \{\tilde{u}(\xi'_n)\} + N_2 [\tilde{u}(\xi'_n)]).$$

We finally write

$$y_j = \sum_m \omega_m |\widehat{DG}|(\xi_m) \sum_{1 \leq i \leq d} \sum_{1 \leq l \leq d} \left((\widehat{DG}^{-1})_{l,i} A_i \tilde{u} \cdot \frac{\partial \tilde{\varphi}_j}{\partial \tilde{x}_l} - B_i (\widehat{DG}^{-1})_{l,i} \frac{\partial \tilde{u}}{\partial \tilde{x}_l} \cdot \tilde{\varphi}_j \right) (\xi_m) \\ + \sum_n \omega'_n |\widehat{Dg}|(\xi'_n) \tilde{U} \cdot \tilde{\varphi}_j(\xi'_n).$$

We decompose this matrix-vector into several stages.

For volume integrals :

1. Evaluate

$$v_m = \tilde{u}(\xi_m) = \sum_k \tilde{u}_k \tilde{\varphi}_k(\xi_m) \\ dv_m^l = \frac{\partial \tilde{u}}{\partial \tilde{x}_l}(\xi_m) = \sum_k \tilde{u}_k \frac{\partial \tilde{\varphi}_k}{\partial \tilde{x}_l}(\xi_m)$$

2. Apply geometry and physics coefficients

$$v_m^{1,l} = \sum_{1 \leq i \leq d} \omega_m |\widehat{DG}|(\xi_m) \widehat{DG}_{l,i}^{-1} A_i v_m \\ v_m^2 = - \sum_{1 \leq i, l \leq d} \omega_m |\widehat{DG}|(\xi_m) B_i \widehat{DG}_{l,i}^{-1} dv_m^l$$

3. Evaluate

$$w_j^1 = \sum_m \sum_{1 \leq l \leq d} v_m^{1,l} \cdot \frac{\partial \tilde{\varphi}_j}{\partial \tilde{x}_l}(\xi_m) \\ w_j^2 = \sum_m v_m^2 \cdot \tilde{\varphi}_j(\xi_m)$$

For surface integral :

1. Evaluate

$$s_n = \sum_k u_k \tilde{\varphi}_k(\xi'_n)$$

2. Apply geometry and physics coefficients to get

$$\bar{s}_n = -(N_1 \{s_n\} + N_2 [s_n]) \\ s_n^1 = \omega'_n |\widehat{Dg}|(\xi'_n) \bar{s}_n$$

3. Evaluate

$$w_j^3 = \sum_n s_n^1 \cdot \tilde{\varphi}_j(\xi'_n)$$

Get the result vector :

$$y_j = w_j^1 + w_j^2 + w_j^3$$

We consider tensorized quadrature points

$$\xi_m = (\xi_{m_1}, \xi_{m_2}, \xi_{m_3})$$

and tensorized basis functions

$$\varphi_j(x, y, z) = \tilde{\varphi}_{j_1}(\tilde{x}) \tilde{\varphi}_{j_2}^{j_1}(\tilde{y}) \tilde{\varphi}_{j_3}^{j_1, j_2}(\tilde{z})$$

We now detail how the different stages containing sums can be decomposed because of tensorization. By performing computations along each coordinate \tilde{x} , \tilde{y} , \tilde{z} , we are able to have sums with only $r + 1$ terms, instead of $(r + 1)^3$ terms if basis functions and quadrature points do not exhibit any tensorization.

3.2.2. Computation of Volume Integrals

1. For $m = (m_1, m_2, m_3)$, we want to evaluate

$$v_m = \sum_{k_1, k_2, k_3} \tilde{\varphi}_{k_1}(\xi_{m_1}) \tilde{\varphi}_{k_2}^{k_1}(\xi_{m_2}) \tilde{\varphi}_{k_3}^{k_1, k_2}(\xi_{m_3}) u_{k_1, k_2, k_3}.$$

We notice $\tilde{\varphi}_{j_3}^{j_1, j_2}$ when the basis function depends on j_1 and j_2 . This triple sum is split into three single sums

$$\begin{aligned} u_{k_1, k_2, m_3}^1 &= \sum_{k_3} \tilde{\varphi}_{k_3}^{k_1, k_2}(\xi_{m_3}) u_{k_1, k_2, k_3} \\ u_{k_1, m_2, m_3}^2 &= \sum_{k_2} \tilde{\varphi}_{k_2}^{k_1}(\xi_{m_2}) u_{k_1, k_2, m_3}^1 \\ v_{m_1, m_2, m_3} &= \sum_{k_1} \tilde{\varphi}_{k_1}(\xi_{m_1}) u_{k_1, m_2, m_3}^2 \end{aligned}$$

Remark 3.1. *At this stage, we observe that the dependency has to be “opposite” between φ_j and ξ_m , otherwise we can not exploit the tensorized structure of quadrature points and basis functions to get fast algorithms. Therefore semi-tensorized quadrature point*

$$\xi_m = (\xi_{m_1}^{m_2, m_3}, \xi_{m_2}^{m_3}, \xi_{m_3})$$

could also be considered.

The three sums involve only $O(r)$ terms and are computed for $O(r^3)$ values, leading to a cost in $O(r^4)$. Each of these sums can be interpreted as a matrix vector product, i.e.

$$\begin{aligned} U^1 &= C_1 U \\ U^2 &= C_2 U^1 \\ V &= C_3 U^2 \end{aligned}$$

We have found a factorization of matrix C

$$C_{m, k} = \tilde{\varphi}_k(\xi_m)$$

which is

$$C = C_3 C_2 C_1$$

While matrix C is dense, the matrices C_3 , C_2 and C_1 are sparse. Matrices C_3 , C_2 , C_1 are independent from the geometry, and are precomputed once for each reference element. Hence, we have

$$V = C U$$

For $n = n_1, n_2, n_3$, we now want to evaluate

$$dv_n^l(\xi_n) = \sum_k \tilde{u}_k \frac{\partial \tilde{\varphi}_k}{\partial \tilde{x}_l}(\xi_n)$$

Since for all elements, we have the inclusion $\tilde{V}_r \subset \mathbb{Q}_r$, we can write

$$\tilde{u}(x, y, z) = \sum_k \tilde{u}_k \tilde{\varphi}_k(\tilde{x}, \tilde{y}, \tilde{z}) = \sum_{m_1, m_2, m_3} v_{m_1, m_2, m_3} \psi_{m_1}(\tilde{x}) \psi_{m_2}(\tilde{y}) \psi_{m_3}(\tilde{z})$$

where $\psi_{m_1}, \psi_{m_2}, \psi_{m_3}$ are Lagrange interpolation basis function associated respectively with points ξ_{m_1}, ξ_{m_2} and ξ_{m_3}

$$\begin{aligned} \psi_{m_1}(\tilde{x}) &= \frac{\prod_{n_1 \neq m_1} \tilde{x} - \xi_{n_1}}{\prod_{n_1 \neq m_1} \xi_{m_1} - \xi_{n_1}} \\ \psi_{m_2}(\tilde{y}) &= \frac{\prod_{n_2 \neq m_2} \tilde{y} - \xi_{n_2}}{\prod_{n_2 \neq m_2} \xi_{m_2} - \xi_{n_2}} \\ \psi_{m_3}(\tilde{z}) &= \frac{\prod_{n_3 \neq m_3} \tilde{z} - \xi_{n_3}}{\prod_{n_3 \neq m_3} \xi_{m_3} - \xi_{n_3}} \end{aligned}$$

We have

$$\tilde{\nabla} \psi_{m_1}(x) \psi_{m_2}(y) \psi_{m_3}(z) = \begin{cases} \sum_{m_1, m_2, m_3} v_{m_1, m_2, m_3} \frac{d\psi_{m_1}}{dx}(\tilde{x}) \psi_{m_2}(\tilde{y}) \psi_{m_3}(\tilde{z}) \\ \sum_{m_1, m_2, m_3} v_{m_1, m_2, m_3} \psi_{m_1}(\tilde{x}) \frac{d\psi_{m_2}}{dy}(\tilde{y}) \psi_{m_3}(\tilde{z}) \\ \sum_{m_1, m_2, m_3} v_{m_1, m_2, m_3} \psi_{m_1}(\tilde{x}) \psi_{m_2}(\tilde{y}) \frac{d\psi_{m_3}}{dz}(\tilde{z}) \end{cases}$$

Since we have

$$\psi_{m_1}(\xi^{n_1}) = \delta_{m_1, n_1}, \quad \psi_{m_2}(\xi^{n_2}) = \delta_{m_2, n_2}, \quad \psi_{m_3}(\xi^{n_3}) = \delta_{m_3, n_3}$$

Triple sums over m_1, m_2, m_3 are reduced to single sums

$$\begin{aligned} \left(\frac{\partial v}{\partial \tilde{x}} \right)_{n_1, n_2, n_3} &= \sum_{m_1} \frac{d\psi^{m_1}}{d\tilde{x}}(\xi_{n_1}) v_{m_1, n_2, n_3} \\ \left(\frac{\partial v}{\partial \tilde{y}} \right)_{n_1, n_2, n_3} &= \sum_{m_2} \frac{d\psi^{m_2}}{d\tilde{y}}(\xi_{n_2}) v_{n_1, m_2, n_3} \\ \left(\frac{\partial v}{\partial \tilde{z}} \right)_{n_1, n_2, n_3} &= \sum_{m_3} \frac{d\psi^{m_3}}{d\tilde{z}}(\xi_{n_3}) v_{n_1, n_2, m_3} \end{aligned}$$

These operations can be viewed as matrix vector product

$$dV = RV$$

where the matrix R is sparse and independent from the geometry, and can be precomputed once for each reference element.

Eventually, we have exhibited the following factorization

$$dV = RCU.$$

2. We compute

$$\begin{aligned} v_m^{1,l} &= \sum_{1 \leq i \leq d} \omega_m |\widetilde{DG}|(\xi_m) \widetilde{DG}_{l,i}^{-1} A_i v_m \\ v_m^2 &= \sum_{1 \leq i \leq d} \omega_m |\widetilde{DG}|(\xi_m) B_i \left(\sum_{1 \leq l \leq d} \widetilde{DG}_{l,i}^{-1} dv_m^l \right) \end{aligned}$$

The complexity of this operation is in $O(r^3)$, and can be viewed as a matrix-vector product

$$\begin{aligned} V^1 &= A V \\ V^2 &= B dV \end{aligned}$$

where matrices A and B are block-diagonal, each block being related to a quadrature point, and depend on the geometry.

3. We are interested in the stage

$$w_j^1 = \sum_{m,l} v_m^{1,l} \cdot \frac{\partial \tilde{\varphi}_j}{\partial \tilde{x}_l}(\xi_m)$$

which is the transpose operation to the computation of derivative of basis functions on quadrature points. Therefore, we have

$$W^1 = C^* R^* V^1$$

We are now interested in the step

$$w_j^2 = \sum_m v_m^2 \cdot \tilde{\varphi}_j(\xi_m)$$

which can be interpreted as

$$W^2 = C^* V^2$$

that is

$$W^2 = C_1^* C_2^* C_3^* V^2$$

Remark 3.2. For hexahedra, using the basis functions of Equation 2.1, the matrix C used to compute u on quadrature points in the fast matrix-vector product is equal to identity

$$C = I.$$

This makes computations faster for hexahedra, that is why we want to have high percentage of hexahedra in a mesh.

3.2.3. Computation of Surface Integrals

1. We are interested in the stage

$$s_p = \tilde{u}(\xi'_p) = \sum_k \tilde{u}_k \tilde{\varphi}_k(\xi'_p)$$

Since we are considering faces of the cube, we have three families of quadrature points

$$\begin{aligned} &(\delta, \xi'_{p_2}, \xi'_{p_3}) \\ &(\xi'_{p_1}, \delta, \xi'_{p_3}) \\ &(\xi'_{p_1}, \xi'_{p_2}, \delta) \end{aligned}$$

δ is equal to 0 or 1. The starting point is to consider the expansion with basis functions of the cube, ie

$$\tilde{u}(\tilde{x}, \tilde{y}, \tilde{z}) = \sum_{m_1, m_2, m_3} v_{m_1, m_2, m_3} \psi_{m_1}(\tilde{x}) \psi_{m_2}(\tilde{y}) \psi_{m_3}(\tilde{z})$$

Then we evaluate u on the families of points

$$\begin{aligned} u_{m_2, m_3}^1 &= \tilde{u}(\delta, \xi_{m_2}, \xi_{m_3}) \\ u_{m_1, m_3}^2 &= \tilde{u}(\xi_{m_1}, \delta, \xi_{m_3}) \\ u_{m_1, m_2}^3 &= \tilde{u}(\xi_{m_1}, \xi_{m_2}, \delta) \end{aligned}$$

These operations consist of single sums

$$\begin{aligned} u_{m_2, m_3}^1 &= \sum_{m_1} \psi_{m_1}(\delta) v_{m_1, m_2, m_3} \\ u_{m_1, m_3}^2 &= \sum_{m_2} \psi_{m_2}(\delta) v_{m_1, m_2, m_3} \\ u_{m_1, m_2}^3 &= \sum_{m_3} \psi_{m_3}(\delta) v_{m_1, m_2, m_3} \end{aligned}$$

which can be interpreted as matrix vector products with sparse matrices P_1, P_2, P_3

$$U^1 = P_1 V, \quad U^2 = P_2 V, \quad U^3 = P_3 V$$

Then, if the first face is a quadrangular face, we can split the computation

$$s_{p_2, p_3}^1 = \sum_{m_2, m_3} \psi_{m_2}(\xi'_{p_2}) \psi_{m_3}(\xi'_{p_3}) u_{m_2, m_3}^1$$

into two stages

$$\begin{aligned} z_{m_2, p_3} &= \sum_{m_3} \psi_{m_3}(\xi'_{p_3}) u_{m_2, m_3}^1 \\ s_{p_2, p_3}^1 &= \sum_{m_2} \psi_{m_2}(\xi'_{p_2}) z_{m_2, p_3} \end{aligned}$$

which can be interpreted as matrix vector products with sparse matrices

$$S^1 = T_2 T_1 U^1$$

If the first face is a triangle, since we are using symmetric quadrature points for triangles [30], which are not tensorized, we only have

$$S^1 = T U^1$$

where matrix T is dense, but only restricted to the face. Therefore the complexity of computation of s_p is in $O(r^3)$ if the element is an hexahedron (only quadrangular faces) and in $O(r^4)$ for other elements, because of the presence of triangular faces. Of course, for other elements, some faces of the cube are not treated since they are reduced to a single point in the real element K . For pyramids, the face $z = 1$ is not treated.

2. We compute

$$\bar{s}_n = -(N_1 \{s_n\} + N_2 [s_n])$$

$$s_n^1 = \omega'_n |\widetilde{Dg}|(\xi'_n) \bar{s}_n$$

3. We are interested in the stage:

$$w_j^3 = \sum_n s_n^1 \cdot \tilde{\varphi}_j(\xi_n')$$

This stage is exactly the transpose operation to the computation of s_n , therefore the computation of w^3 is done by using transpose of matrices defined in the previous subsection (matrices P_1, P_2, P_3, T_1, T_2).

3.3. With Warburton's Trick

Using the transformation 2.6, the stiffness matrix is transformed into

$$\begin{aligned} (R_h)_{j,k} &= \int_{\hat{K}} |DF| \sum_{1 \leq i \leq d} A_i \frac{\partial(\frac{\hat{\varphi}_k}{\sqrt{|DF|}})}{\partial x_i} \cdot \frac{\hat{\varphi}_j}{\sqrt{|DF|}} d\hat{x} - \int_{\hat{K}} |DF| \sum_{1 \leq i \leq d} B_i \frac{\hat{\varphi}_k}{\sqrt{|DF|}} \cdot \frac{\partial(\frac{\hat{\varphi}_j}{\sqrt{|DF|}})}{\partial x_i} d\hat{x} \\ &= \int_{\hat{K}} \sum_{1 \leq i \leq d} A_i \frac{\partial \hat{\varphi}_k}{\partial x_i} \cdot \hat{\varphi}_j d\hat{x} - \int_{\hat{K}} \sum_{1 \leq i \leq d} B_i \varphi_k \cdot \frac{\partial \hat{\varphi}_j}{\partial x_i} d\hat{x} \\ &\quad + \frac{1}{2} \int_{\hat{K}} \sum_{1 \leq i \leq d} (B_i - A_i) \frac{1}{|DF|} \frac{\partial |DF|}{\partial x_i} \hat{\varphi}_k \cdot \hat{\varphi}_j d\hat{x} \end{aligned}$$

We can use the fast matrix vector product detailed above with this modified stiffness matrix without important overcost. Moreover, since the mass matrix is equal to identity, this leads to faster computations as shown in Table 4.10. However, the stiffness matrix involves the derivative of jacobian and this has to be treated carefully with pyramids. Indeed, for non-affine pyramids, the derivative of jacobian is singular :

$$\frac{\partial |DF|}{\partial \hat{x}} = B_1 \frac{1}{1 - \hat{z}} + C \frac{\hat{y}}{(1 - \hat{z})^2} = B_1 \frac{1}{1 - \hat{z}} + C \frac{2\hat{y} - 1}{1 - \hat{z}}$$

Therefore, it is preferable, for volume integrals, to use Gauss-Jacobi quadrature formula exact for polynomials in $(1 - \hat{z})\mathbb{Q}_r$ instead of $(1 - \hat{z})^2\mathbb{Q}_r$ as chosen classically for pyramids.

4. Comparison of Several Types of Elements

Experiments to compare the elements previously constructed are conducted on Maxwell's equations.

For Maxwell's equations, $d = 3$ and $n_s = 6$ where u^m is E_x, E_y, E_z, H_x, H_y or H_z . The system is the following for E and H in \mathbb{R}^3

$$\begin{cases} \frac{dE}{dt} - \text{rot}H = 0 \\ \frac{dH}{dt} + \text{rot}E = 0 \end{cases} \quad (4.1)$$

that is

$$M = \begin{pmatrix} \varepsilon & 0 & 0 & 0 & 0 & 0 \\ 0 & \varepsilon & 0 & 0 & 0 & 0 \\ 0 & 0 & \varepsilon & 0 & 0 & 0 \\ 0 & 0 & 0 & \mu & 0 & 0 \\ 0 & 0 & 0 & 0 & \mu & 0 \\ 0 & 0 & 0 & 0 & 0 & \mu \end{pmatrix},$$

and

$$A_1 = \begin{pmatrix} 0 & 0 & 0 & 0 & 0 & 0 \\ 0 & 0 & 0 & 0 & 0 & 0 \\ 0 & 0 & 0 & 0 & 0 & 0 \\ 0 & 0 & 0 & 0 & 0 & 0 \\ 0 & 0 & -1 & 0 & 0 & 0 \\ 0 & 1 & 0 & 0 & 0 & 0 \end{pmatrix}, \quad A_2 = \begin{pmatrix} 0 & 0 & 0 & 0 & 0 & 0 \\ 0 & 0 & 0 & 0 & 0 & 0 \\ 0 & 0 & 0 & 0 & 0 & 0 \\ 0 & 0 & 1 & 0 & 0 & 0 \\ 0 & 0 & 0 & 0 & 0 & 0 \\ -1 & 0 & 0 & 0 & 0 & 0 \end{pmatrix}, \quad A_3 = \begin{pmatrix} 0 & 0 & 0 & 0 & 0 & 0 \\ 0 & 0 & 0 & 0 & 0 & 0 \\ 0 & 0 & 0 & 0 & 0 & 0 \\ 0 & -1 & 0 & 0 & 0 & 0 \\ 1 & 0 & 0 & 0 & 0 & 0 \\ 0 & 0 & 0 & 0 & 0 & 0 \end{pmatrix}.$$

The matrices B_i are obtained by taking the transpose of A_i .

4.1. Hexahedron

The orthogonal base of Proposition 2.1 provides a diagonal mass matrix for non-affine hexahedra, while the tensorial product of Legendre polynomials proposed by Kirby *et al.* [14] (with $P_1 = P_2 = P_3 = r$) and Warburton [29] only provides mass-lumping for affine elements.

When the hexahedron is affine, we use the basis functions of Proposition 2.2. We write derivative of Legendre polynomials as

$$\frac{dP_i^{0,0}}{dx}(x) = \sum_{j=0}^{i-1} \eta_j^i P_j^{0,0}(x)$$

Because of orthogonality, for an affine hexahedron, we have

$$\begin{aligned} \int_{\hat{K}} \frac{\partial \varphi_{i_1, i_2, i_3}}{\partial \hat{x}} \varphi_{j_1, j_2, j_3} dx &= \eta_{j_1}^{i_1} \delta_{i_2, j_2} \delta_{i_3, j_3} \\ \int_{\hat{K}} \frac{\partial \varphi_{i_1, i_2, i_3}}{\partial \hat{y}} \varphi_{j_1, j_2, j_3} dx &= \eta_{j_2}^{i_2} \delta_{i_1, j_1} \delta_{i_3, j_3} \\ \int_{\hat{K}} \frac{\partial \varphi_{i_1, i_2, i_3}}{\partial \hat{z}} \varphi_{j_1, j_2, j_3} dx &= \eta_{j_3}^{i_3} \delta_{i_1, j_1} \delta_{i_2, j_2} \end{aligned}$$

This stiffness matrix is sparser and smaller than the stiffness matrix used for \mathbb{Q}_r . The asymptotic cost of the product with stiffness matrix will be in r^4 whereas it will be in $12r^4$ for \mathbb{Q}_r . However, the flux part remains expensive (even though in $O(r^3)$) since for example for face $x = 0$, we get

$$u(0, \hat{y}, \hat{z}) = \sum_{i_1, i_2, i_3} u_{i_1, i_2, i_3} P_{i_1}^{0,0}(-1)$$

Therefore we can write value of solution s on this face by using Legendre expansion

$$s(\hat{y}, \hat{z}) = \sum_{i_2, i_3} s_{i_2, i_3} P_{i_2}^{0,0}(\hat{y}) P_{i_3}^{0,0}(\hat{z})$$

We obtain S with the following matrix vector product

$$S = PU$$

where

$$P_{(i_2, i_3), (j_1, j_2, j_3)} = P_{j_1}^{0,0}(-1) \delta_{i_2, j_2} \delta_{i_3, j_3}$$

This matrix contains $\frac{1}{6}(r+1)(r+2)(r+3)$ elements. Since Legendre expansion of s is orthonormal on each square composing the boundary of the cube, there is no quadrature rule

Table 4.1: Computational time spent for 100 iterations with a mesh containing 1 million dofs for unknown E_x .

Order	2	3	4	5	6	7	8	10	12	15
\mathbb{Q}_r	136s	111s	107s	100s	101s	99s	109s	105s	113s	140s
\mathbb{P}_r	214s	157s	135s	117s	111s	105s	106s	101s	97s	99s

involved for fluxes terms. One would expect much more efficient computations by using this base, but since the number of degrees of freedom of \mathbb{P}_r is lower than for \mathbb{Q}_r , one needs much finer mesh to have the same number of degrees of freedom. Thus, when we compare the computation time for one million degrees of freedom in Table 4.1, we obtain almost the same cost for \mathbb{P}_r and \mathbb{Q}_r . However, for \mathbb{P}_r , the cost remains constant for higher orders than for \mathbb{Q}_r .

For a sharper comparison, we study the L^2 -error obtained for a cubic cavity meshed with small cubes. Because of symmetry, only the cube $[0, 5\lambda]^2$ is meshed. In Tables 4.2 and 4.3, we measure the minimal computational time and minimal number of degrees of freedom necessary to obtain an error less than 1%, for \mathbb{P}_r and \mathbb{Q}_r .

Table 4.2: Time step, number of dofs and computational time necessary to reach an error level below one percent for a cubic cavity (affine mesh). Use of \mathbb{P}_r on hexahedra with Legendre orthogonal expansion.

Order	3	4	5	6	8	10	14	18	26
Δt	0.035	0.0405	0.0394	0.0395	0.0348	0.0325	0.0272	0.0235	0.0179
Dofs	540 000	240 065	153 664	111 804	84 480	61 776	43 520	35 910	29 232
CPU Time	11 818s	2865s	1387s	856s	695s	500s	444s	376s	620s

Table 4.3: Time step, number of dofs and computational time necessary to reach an error level below one percent for a cubic cavity (affine mesh). Use of \mathbb{Q}_r on hexahedra with Lagrange interpolation functions base on Gauss-Legendre points.

Order	3	4	5	6	7	9	11	16	30
Δt	0.032	0.036	0.0353	0.0344	0.0381	0.0315	0.0301	0.023	0.0156
Dofs	512 000	216 000	157 464	117 649	64 000	64 000	46 656	39 304	29 791
CPU Time	5 575s	1800s	1180s	1013s	417s	580s	426s	1134s	3520s

It seems better to use \mathbb{P}_r than \mathbb{Q}_r for higher orders, but all in all, the two methods give similar computational times. We think that using \mathbb{Q}_r is a better choice than using \mathbb{P}_r since the method also works for non-affine hexahedron, which means implementing a single method for all the cases.

4.2. Wedges

The orthogonal basis functions of Proposition 2.1 are almost the same as Kirby *et al.* [14] and Warburton [29], except that we take Lagrange interpolation functions with Gauss points

instead of Legendre polynomials in z . For nodal functions, we actually have a tensorization in z , leading to a matrix-vector product in $O(r^5)$ instead of $O(r^4)$ for orthogonal basis. In Table 4.4, the computational times given by both basis are very close, orthogonal functions provide faster computations from order 5.

Table 4.4: Time spent for 100 iterations for meshes of non-affine wedges containing one million dofs for E_x .

Order	2	3	4	5	6	7	8
Nodal	296	312	239	342	343	353	400
Orthogonal	338	326	280	315	292	317	361

We have conducted similar experiments than for affine-hexahedron, in order to compare the use of \mathbb{P}_r and the use of the optimal finite element space for wedges. For \mathbb{P}_r , we take the orthogonal basis functions of Proposition 2.2. The required number of degrees of freedom and computational time for the experiments can be read in tables 4.5 and 4.6.

Table 4.5: Time step, number of dofs and computational time necessary to reach an error level below one percent for a cubic cavity (affine mesh). Use of \mathbb{P}_r on prisms with orthogonal expansion.

Order	3	4	5	6	7	8	9
Δt	0.0268	0.0296	0.0309	0.029	0.0285	0.0268	0.0258
Dofs	351 520	172 955	96 768	84 000	61 440	56 595	47 520
Computation Time	30 330s	12 920s	7 145s	7028s	5 560s	6 306s	6 602s

Table 4.6: Time step, number of dofs and computational time necessary to reach an error level below one percent for a cubic cavity (affine mesh). Use of optimal finite element space on prisms.

Order	3	4	5	6	7	8	9
Δt	0.0277	0.0306	0.031	0.0298	0.0268	0.025	0.025
Dofs	425 920	205 800	126 000	100 352	98 784	87 480	68 750
Computation Time	22 020s	6 834s	3 904s	3 340s	3 930s	4 397s	3 727s

In this case, we do not have the same advantage than for hexahedra where quadrature-free algorithms lead to faster computations. The use of optimal finite element space is then much better, even though the number of degrees of freedoms is lower for \mathbb{P}_r .

4.3. Pyramids

Computations are done for a mesh containing only non-affine pyramids and with one million degrees of freedom for unknown E_x . In Table 4.7, we compare the CPU time spent for the computation and Cholesky factorization of mass matrix for nodal functions and orthogonal basis, using the algorithm previously described. The computational time needed for nodal

functions grows very quickly, making the use of orthogonal functions very attractive when r is high.

Table 4.7: Time to compute and invert mass matrix

Order	2	3	4	5	6	7	8
Dense Matrix	1.91s	7.98s	26.2s	73.6s	177s	391s	786s
Sparse Matrix	0.577s	0.98s	1.32s	2.27s	4.08s	5.17s	7.62s

In Table 4.8, we display the ratio between the amount of memory used for a dense and a sparse mass matrix with orthogonal basis. The induced gain of storage is quite interesting for both the matrix and its Cholesky factorisation.

Table 4.8: Gain in storage for the matrix and its Cholesky factorization by using orthogonal functions instead of nodal functions

Order	2	3	4	5	6	7	8
Gain for matrix	1.81	2.94	4.46	6.38	8.7	11.4	14.6
Gain for factorization	1.52	1.91	2.39	2.83	3.38	3.85	4.8

We finally perform a comparison between different solvers to invert the mass matrix: a dense solver, a sparse solver and an iterative solver using fast matrix vector product deduced from expression of mass matrix given in Section 2.1. As shows Table 4.9, the sparse solver outperforms the other solvers. The main drawback of iterative solver is the relatively high number of iterations since it needed 10 iterations to get a residual less than 10^{-12} .

We compare the computation time spent for 100 iterations with a mesh made of non-affine pyramids only with one million dofs in Table 4.10. The efficiency of the product seems quite interesting, since with Warburton's trick, the cost remains almost constant (between 400 and 500s here) versus the order of approximation. When a sparse solver is used, the additional overcost is quite acceptable if a high accuracy is sought. The cost of the matrix vector product using nodal functions (with quadrature too) becomes quickly prohibitive when r is large enough. We observe in this table a gain in time by using orthogonal functions from order 3.

Similar experiments to the one conducted for affine hexahedron are done to compare \mathbb{P}_r and the optimal finite element space for pyramids. For \mathbb{P}_r , we take the orthogonal basis functions of Proposition 2.2, which is the base proposed by Kirby *et al.* [14].

The required number of degrees of freedom and computational time can be read in tables 4.11 and 4.12.

Table 4.9: Comparison of iterative solver, sparse solver, dense solver

Order	2	3	4	5	6	7	8
Dense Solver	91s	144s	183s	295s	340s	503s	652s
Iterative Solver	150s	150s	149s	331s	366s	403s	439s
Sparse Solver	74s	101s	121s	148s	178s	227s	235s

Table 4.10: Time spent for 100 iterations for meshes of non-affine pyramids containing one million dofs for E_x .

Order	2	3	4	5	6	7	8
Sparse solver	523s	505s	508s	569s	619s	692s	766s
Warburton trick	460s	432s	411s	451s	471s	494s	548s
Nodal functions	378s	532s	702s	1135s	2425s	7618s	15350s

Table 4.11: Time step, number of dofs and computational time necessary to reach an error level below one percent for a cubic cavity (affine mesh). Use of \mathbb{P}_r on pyramids with orthogonal expansion.

Order	3	4	5	6	7	8	9
Δt	0.0238	0.0258	0.0248	0.024	0.0216	0.0205	0.0203
Dofs	960 000	461 370	336 000	258 048	246 960	213 840	165 000
Computation Time	60 449s	27 564s	22 422s	19 111s	21 433s	22 074s	19 056s

Table 4.12: Time step, number of dofs and computational time necessary to reach an error level below one percent for a cubic cavity (affine mesh). Use of optimal finite element space on pyramids.

Order	3	4	5	6	7	8
Δt	0.0276	0.0307	0.028	0.0285	0.0268	0.0268
Dofs	737 280	330 000	279 552	181 440	153 000	109 440
Computation Time	28 267s	10 898s	10 800s	7 246s	6 933s	5 204s

We observe that the optimal finite element space is more efficient even on affine pyramids, since the computational time required for eighth-order is 5 204s for optimal space, and 19 056s for polynomials.

4.4. Tetrahedra

For tetrahedra, the use of orthogonal functions is known to be not very attractive for low orders, as noticed by Warburton [29]. In Table 4.13, we report computational times obtained for different orders of approximation with both nodal and orthogonal bases functions. We check that nodal basis functions provide faster algorithms when $r < 10$. We use quadrature-free algorithms as described in Hesthaven and Warburton [1] to evaluate the integrals.

Table 4.13: Time spent for 100 iterations of leap frog-scheme for meshes containing one million dofs for E_x . Affine tetrahedra

Order	2	3	4	5	6	7	8	9	10
Nodal	379s	358s	327s	343s	428s	541s	680s	1023s	1751s
Orthogonal	527s	601s	559s	595s	679s	722s	798s	992s	1074s

5. Applications to Maxwell's Equations

5.1. Convergence for a Cubic Cavity

We consider time-domain Maxwell's equations in a cubic cavity $[-5, 5]^3$ with a gaussian source

$$f = x e^{-\alpha x^2} e_x$$

with a mesh containing non-affine pyramids (see Fig 1.2).

The solutions for $T = 5$ and $T = 50$ are displayed on Fig. 5.1. An error analysis is performed for the solution obtained at $T = 50s$ for orders 3 and 5 by using the sparse solver to compute the mass matrix or Warburton's trick. As shows Fig. 5.2, as expected, this trick does not provide a h -convergent scheme, whereas the h -convergence is ensured with our method. However, we may conjecture that Warburton's trick does provide a p -convergent scheme, since the error of consistency is decreasing when we use order 5 instead of order 3. Moreover, the level of consistency error (less than 2%) is quite acceptable in most of simulations.

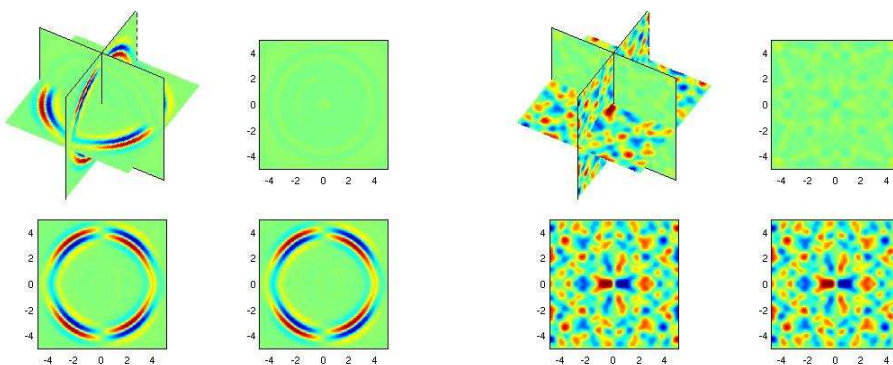


Fig. 5.1. Cube of size 10λ - Solution for $T = 5$ (left) and $T = 50$ (right)

5.2. Air Balloon

We consider the scattering of an air balloon in a parallelepiped box $[-250, 50] \times [-130, 180] \times [90, 490]$, with the following source

$$f(x, t) = e^{-13.8(\frac{r}{r_0})^2} e^{-0.001(t-t_0)^2} \sin(2\pi f_0 t)$$

where $r_0 = 15$, $f_0 = 0.08$. The hybrid mesh used for the experiment, chosen to provide an L^2 -error below one percent with \mathbb{Q}_5 approximation, is presented on Fig. 5.3

For this experiment, we use the classical leap-frog scheme for the time discretization. In Fig. 5.4 is displayed the E_x component of the numerical solution obtained for $T = 288$ and $T = 432$. Since we do not have a curved mesh, we compare each solution to a numerical solution computed on the same mesh but with an order of approximation equal to $r + 1$ instead of r . In Table 5.1, we detail the computational time needed to reach an L^2 error lower than one percent.

Numerical experiments have been completed on 256 processors, computational times are obtained by summing the CPU time spent on each processor and subtracting the cost of communications.

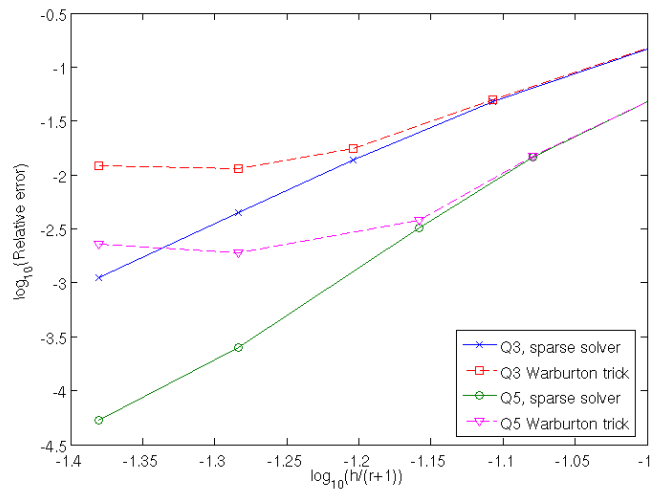


Fig. 5.2. Relative L^2 error obtained on deformed hybrid mesh (tetras+pyramids) - Cube of size 10λ - Fourth-order low-storage Runge-Kutta scheme

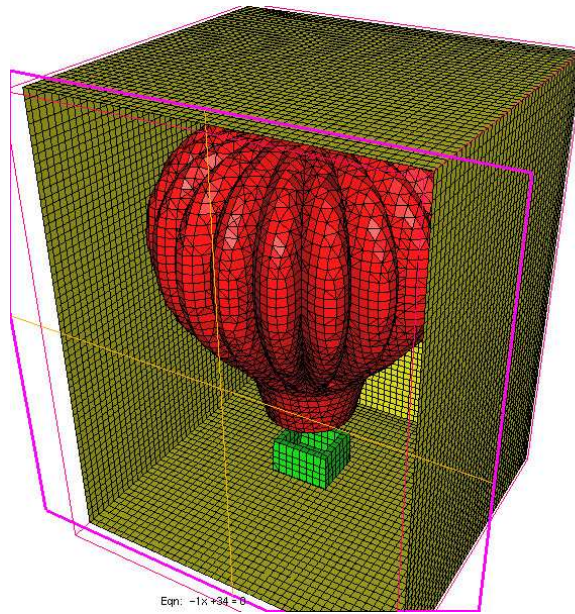


Fig. 5.3. Hybrid mesh used for the computations of the scattering of an air balloon.

Conclusion

Highly efficient pyramidal elements of any order have been constructed for discontinuous Galerkin methods. Numerical experiments conducted with these elements on Maxwell's equations showed a very good behaviour with hybrid meshes.

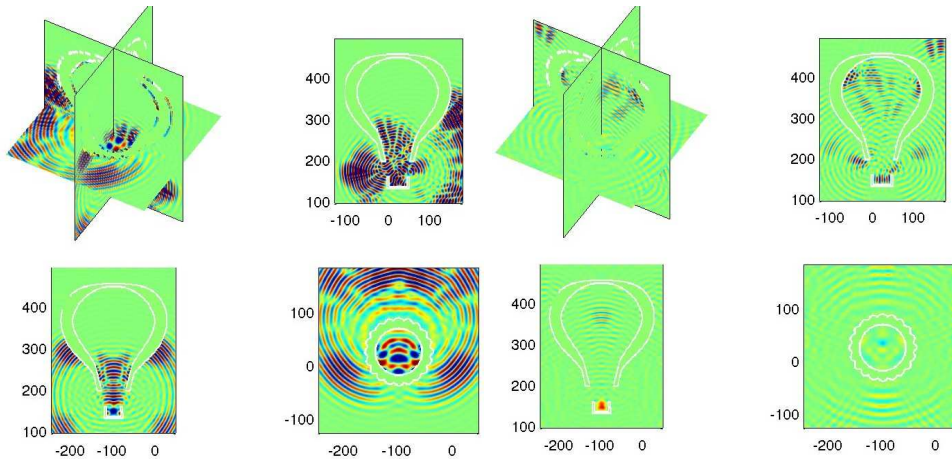


Fig. 5.4. Solution obtained for $T = 288$ (top) and $T = 432$ (bottom).

Table 5.1: Number of degrees of freedom and computational time needed to reach an L^2 -error of 1% with fifth order approximation, for $T = 432s$ - Leap-frog scheme

Mesh used	L^2 -error	Nb of dofs	Δt	CPU Time	
				Nodal	Ortho
Hybrid	0.0093	22.4 millions	0.032	4d 2h 36min	3d 17h 2min
Tetrahedral	0.011	37.9 millions	0.046	11d 10h 19min	-

References

- [1] J. Hesthaven and T. Warburton, High order discontinuous Galerkin methods for the Maxwell eigenvalue problem, *Philos. Trans. R. Soc. Lond. Ser. A Math. Phys. Eng. Sci.*, **1816** (2004), 493–524.
- [2] G. Cohen and S. Fauqueux, Mixed finite elements with mass-lumping for the transient wave equation, *Journal of Computational Acoustics*, **8** (2000), 171–188.
- [3] G. Cohen, X. Ferrieres and S. Pernet, A spatial high-order hexahedral discontinuous Galerkin method to solve Maxwell equations in time domain, *Journal of Computational Physics*, **217** (2006), 340–363.
- [4] S. Pernet and X. Ferrieres, hp a-priori error estimates for a non-dissipative spectral discontinuous galerkin method to solve the maxwell equations in the time domain, *Mathematics of Computation*, **76** (2007), 1801–1832.
- [5] M. Duruflé, Intégration numérique et éléments finis d'ordre élevé appliqués aux équations de Maxwell en régime harmonique., PhD thesis, Université Paris IX-Dauphine, 2006.
- [6] M. Duruflé, P. Grob and P. Joly, Influence of the gauss and gauss-lobatto quadrature rules on the accuracy of a quadrilateral finite element method in the time domain, *Numerical Methods for Partial Differential Equations*, **25** (2009), 526–551.
- [7] L. Demkowicz, J. Kurtz, D. Pardo, M. Paszynski, W. Rachowicz and A. Zdunek, Computing With hp-Adaptive Finite Element, Volume II, Chapman and Hal, 2007.
- [8] N. Nigam and J. Phillips, Higher-order finite elements on pyramids, Technical report, 2007.
- [9] N. Nigam and J. Phillips, Numerical integration for high order pyramidal finite elements, Technical report, 2010.

- [10] M. Bergot, G. Cohen and M. Duruflé, Higher-order finite elements for hybrid meshes using new nodal pyramidal elements, *Journal of Scientific Computing*, **42**:3 (2010), 345–381.
- [11] S. Sherwin, T. Warburton and G. Karniadakis, Spectral/hp methods for elliptic problems on hybrid grids, *Contemporary Mathematics*, **218** (1998), 191–216.
- [12] M. Bluck and S. Walker, Polynomial basis functions on pyramidal elements, *Comm. Numer. Meth. Engng.*, **24** (2008), 1827–1837.
- [13] C. Wieners, Conforming discretizations on tetrahedrons, pyramids, prisms and hexahedrons, 1957.
- [14] R. Kirby, T. Warburton, I. Lomtev and G. Karniadakis, A discontinuous galerkin spectral/hp method on hybrid grids, *Applied Numerical Mathematics*, **33** (2000), 393–405.
- [15] G. Gassner, F. Lörcher, C. Munz and J. Hesthaven, Polymorphic nodal elements and their application in discontinuous galerkin methods, *Journal of Computational Physics*, **228**:5 (2009), 1573–1590.
- [16] G. Cohen, Higher-Order Numerical Methods for Transient Wave Equations, Springer Verlag, 2002.
- [17] M.J.S.Chin-Joe-Kong, W. Mulder and M.V. Veldhuizen, Higher-order triangular and tetrahedral finite element with mass lumping for solving the wave equation, *Journal of Engineering Mathematics*, **35** (1999), 405–426.
- [18] M. Costabel and M. Dauge, Weighted regularization of Maxwell equations in polyhedral domains a rehabilitation of nodal finite element, *Numer. Math.*, **93** (2002), 239–277.
- [19] P.R. E. Godlewski, Hyperbolic Systems of Conservation Laws, Ellipses, 1991.
- [20] J. Hesthaven and T. Warburton, High-order nodal methods on unstructured grids. i. time-domain solution of maxwell’s equations, *J. Comput. Phys.*, **181**:1 (2002), 186–221.
- [21] P. Ciarlet, The Finite Element Method for Elliptic Problems, North-Holland, 1978.
- [22] G. Bedrosian, Shape functions and integration formulas for three-dimensional finite element analysis, *International Journal of Numerical Methods in Engineering*, **35** (1992), 95–108.
- [23] S. Pernet, Étude de méthodes d’ordre élevé pour résoudre les équations de Maxwell dans le domaine temporel. Application à la détection et à la compatibilité électromagnétique, PhD thesis, Université de Paris IX Dauphine, 2004.
- [24] H. Carpenter and C.A. Kennedy, Fourth-order 2n-storage runge-kutta schemes, Technical report, NASA Langley Research Center, 1994.
- [25] P. Monk, Finite elements methods for Maxwell’s equations, Oxford Science Publication, 2002, 2002.
- [26] P. Hammer, O. Marlowe and A. Stroud, Numerical integration over simplexes and cones, *Mathematical Tables and Other Aids to Computation*, **10**:55 (1956), 130–137.
- [27] G. Szegő, Orthogonal Polynomials - Ch. 4 Jacobi Polynomials, 4th ed Amer. Math. Soc., Providence, RI, 1975.
- [28] P. Amestoy, T.A. Davis and I.S. Duff, Algorithm 837 - amd, an approximate minimum degree ordering algorithm, *ACM Transactions on Mathematical Software*, **30**:3 (2004), 381–388.
- [29] T. Warburton, Spectral/hp Methods on Polymorphic Multi-Domains: Algorithms and Applications, PhD thesis, Brown University, 1999.
- [30] D. Dunavant, High degree efficient symmetrical gaussian quadrature rules for the triangle, **21** (1985), 1129–1148.